

Machine Learning Approach to Uncovering Residential Energy Consumption Patterns Based on Socioeconomic and Smart Meter Data

Wenjun Tang^a, Hao Wang^{b,c,*}, Xian-Long Lee^d, Hong-Tzer Yang^{d,*}

^aSmart Grid & Renewable Energy Lab, Tsinghua Berkeley Shenzhen Institute, Shenzhen 518055

^bDepartment of Data Science and AI, Faculty of Information Technology, Monash University, Melbourne, VIC 3800, Australia

^cMonash Energy Institute, Monash University, Melbourne, VIC 3800, Australia

^dDepartment of Electrical Engineering, National Cheng Kung University, Tainan 70101

Abstract

The smart meter data analysis contributes to better planning and operations for the power system. This study aims to identify the drivers of residential energy consumption patterns from the socioeconomic perspective based on the consumption and demographic data using machine learning. We model consumption patterns by representative loads and reveal the relationship between load patterns and socioeconomic characteristics. Specifically, we analyze the real-world smart meter data and extract load patterns by clustering in a robust way. We further identify the influencing socioeconomic attributes on load patterns to improve our method's interpretability. The relationship between consumers' load patterns and selected socioeconomic features is characterized via machine learning models. The findings are as follows. (1) Twelve load clusters, consisting of six for weekdays and six for weekends, exhibit a diverse pattern of lifestyle and a difference between weekdays and weekends. (2) Among various socioeconomic features, age and education level are suggested to influence the load patterns. (3) Our proposed analytical model using feature selection and machine learning is proved to be more effective than XGBoost and conventional neural network model in mapping the relationship between load patterns and socioeconomic features.

Keywords: Consumption Pattern, Socioeconomic, Smart Meter, Clustering, Feature Selection, Machine Learning

Nomenclature

Sets and Indices

$\hat{\mathcal{C}}_w, \hat{\mathcal{C}}_e$ The set of profile indices in each cluster

\mathcal{N} Consumer set

\mathcal{S} The set of socioeconomic features

\mathcal{S}^k The selected subset of feature(s)

\mathcal{S}^k The subset of socioeconomic features

\mathcal{U}, \mathcal{V} Feature index

e Index of weekend

w Index of weekday

d Index of day

t Index of time

Parameters

B_i^k The bias matrix of neural network

w_l^k The weight matrix of neural network

D Total number of days

K Number of the load cluster

Variables

\hat{L}_w, \hat{L}_e Representative load profiles

$L_{w,d}^n, L_{e,d}^n$ Clustered load profile

o_l^k The output of layer l

$\hat{p}_{k,n}$ The intermediate-result of the prediction

μ_n, ν_n Feature value

$\sigma(\cdot)$ The activation function of neural network

$H(\cdot)$ Entropy

$L_{w,d,t}^n, L_{e,d,t}^n$ Normalized load profile

$l_{w,d,t}^n, l_{e,d,t}^n$ Original load profile

$MI(\cdot)$ Mutual information

$P(\cdot)$ Marginal probabilities

$p_{k,n}$ Load pattern distribution of consumer n

SC Silhouette Coefficient index

*Corresponding authors.

Email addresses: monikatang@sz.tsinghua.edu.cn (Wenjun Tang), hao.wang2@monash.edu (Hao Wang), xlllee@ee.ncku.edu.tw (Xian-Long Lee), htyang@ncku.edu.tw (Hong-Tzer Yang)

$SU(\cdot)$ Symmetric uncertainty

$E_{i,j}$ Euclidean distance measurement

1. Introduction

Widespread deployment of smart meters generated a large volume of electricity consumption data. The newly available data of electricity consumption opened up opportunities for the utility to improve the system operation. Recent works took the perspective of the system operator or the utility to study how to utilize smart meter data analysis to enhance the system planning and operations through load forecasting [1, 2, 3], demand response and customer behavior analysis [4, 5, 6], etc.

Smart meter data analysis provides insights into the electricity consumption patterns and characterizes consumption behaviors using load clustering [7]. From the review of [4], the main applications of smart meter data analytics can be classified into load analysis, load forecasting, and load management. The daily load curve can reflect the activities, e.g., cooking, cleaning, entertainment, and sleeping. The consumption behavior analysis can identify energy-saving potentials, plan energy supply, improve energy efficiency [8], and explore the diversity effect in residential energy consumption [9]. It thus helps the system operator to determine the electricity tariff [10] and select consumers for various energy programs, e.g., demand response (DR) [11] and energy efficiency programs [12]. A lifestyle segmentation method was developed in [13] to facilitate data-driven grid management using consumers' daily load shapes and consumption patterns. Utilizing the characterized consumption behavior, not only the energy management strategy but also the anomaly detection can be made [14]. Instead of focusing on the shape of the load curves, the work in [15] investigated the transitions and relations between consumption behaviors based on the clustering results. Kwac and Rajagopal in [16] formulated a stochastic knapsack problem and utilized clustering results for customer selection in DR programs to minimize operational costs. More detailed literature review is presented in Section 2.

From the discussions above, smart meter data can significantly improve the operation and consumer services of the utility through electricity consumption behavior analysis. Nevertheless, most related works rely on each consumer's historical load data to perform the consumption behavior analysis, which does not provide insights into the drivers of consumption behaviors. Studies in [17] revealed that energy consumption results from complex factors, such as socioeconomic and demographic factors. In addition, some households may not have been equipped with smart meters [18], or no historical data are available for new tenants. A few recent studies [19, 20] took a new perspective to investigate the relationship between energy consumption and socioeconomic features, e.g., characteristics of the occupants. Meanwhile, the household natural gas consumption patterns and their influencing factors are explored using cluster analysis, taking into account the increasing block tariffs and temperature factors [21]. Thanks to the efforts made in the Pecan Street smart grid project, both smart meter data

and household survey data become available [22], enabling our study.

The above discussion motivates us to investigate the relationship between consumers' load patterns and socioeconomic features and improve the understanding of consumption behaviors. In our work, using the real-world load and socioeconomic data, we reveal the electricity consumption patterns of consumers (e.g., using representative load curves), identify the main socioeconomic drivers of consumption patterns, and develop a framework to characterize the relationship between load patterns and socioeconomic features. To the best of our knowledge, our work is among the first to reveal the relationship between daily load patterns and socioeconomic factors using machine learning. We summarize the contributions of this paper as follows.

- *Load Pattern Extraction and Socioeconomic Feature Selection:* Given the advantage of the robustness to outliers and noises in real-world data, we model load patterns using the K-Medoids clustering, obtaining representative load profiles with associated probabilities. We use an entropy-based feature selection algorithm to select the most correlated socioeconomic features with load patterns for enhancing the consumption behavior analysis and interpretability.
- *Tailored Model Using Deep Learning:* We develop an analytical model by constructing pattern-dependent deep neural networks (DNNs) with a normalization layer to indicate the consumer's probability distribution of major load patterns only based on its socioeconomic information.
- *Insights From Real-World Data:* We train and test our developed method based on real-world data. The results show strong correlations between the load patterns and selected socioeconomic features, improving the understanding of impact of socioeconomic factors on consumption behaviors. The evaluation results of load pattern distributions also demonstrate that our method outperforms benchmark methods, such as regression and unified DNN models.

The remainder of this paper is organized as follows. We review the related works in Section 2. We detail the analytical methodology, including clustering, feature selection, and deep learning model, in Section 3. We discuss the simulation results in Section 4 and conclude this paper in Section 5.

2. Literature Review

Load profiling emerges as a promising method to help the system operator and the utility understand the consumption behaviors [13] and enhance the operation and services, such as electricity tariff design [10], consumer selection for demand response (DR) [11], and energy efficiency programs [12]. The essential technique of load profiling is the clustering method, as clustering is an unsupervised learning method and has a great advantage in analyzing large-scale load datasets without labeled

information. Specifically, clustering methods define the groups in an unsupervised way by organizing the data and placing similar objects into homogeneous groups [23]. There are different clustering techniques [24], e.g., partitioning, hierarchical, grid-based, density-based, and feature-based methods, among which partitioning clustering is most widely employed to deal with time-series data. As one of the partitioning clustering methods, K-Means clustering is commonly used for shape-based load patterns due to its versatility on large datasets [4]. However, the conventional K-Means method smooths out the temporal variations and may lose essential features [25]. The K-Means method is also sensitive to the outliers and noises, resulting in narrow class margins among clusters and limitations in the interpretability of centroids [26]. In contrast, the K-Medoids method can overcome the above drawbacks, and thus we use K-Medoids to process the real-world smart meter data.

The socioeconomic information has been shown to contribute to the analysis of energy consumption [19], natural gas consumption [21], and fuel poverty [27]. Through employing the cluster analysis, the work in [21] correlated the household natural gas consumption pattern with the socioeconomic factors, which aims to help improve energy efficiency and policy development. Daily smart meter data, combined with socioeconomic data, can enhance the understanding of energy consumption and the determinants of consuming behavior [27]. Han et al. [28] improved the forecasting performance of peak load and energy consumption by considering socioeconomic factors. The study in [19] showed the relationship between the seasonal load patterns and the socioeconomic information. And the structural and behavioral determinants of residential electricity daily peak and idle consumption can be estimated in a similar manner as well [29]. However, it lacks a systematic approach to understanding the effects of socioeconomic factors on energy consumption behaviors.

Feature selection is proved to be a useful technique to remove the irrelevant and redundant features, improve efficiency and performance of learning tasks, and enhance the interpretability of the results [30]. Three primary types of methods are raised as feature selection algorithms, e.g., filter model, wrapper model, and embedded model [31]. The filter models can be employed to filter out irrelevant or redundant features [32]. The filter model has higher computational efficiency compared with other feature selection models [30]. In our work, we use entropy-based class measurement [33] to identify useful socioeconomic features affecting load patterns.

In the smart grid project conducted by the Pecan Street team [22], household socioeconomic data have been collected through energy audits together with the household consumption data. The collected socioeconomic data enable us to study how the energy customers' socioeconomic characteristics drive the consumption patterns. Recent works in [19, 20, 34] attempted to study the relationship between energy consumption and socioeconomic status, and the preliminary results showed that the peak load and energy consumption are correlated with socioeconomic factors. However, how socioeconomic factors affect residential energy consumption patterns is not well understood. This motivates us to develop a systematic framework to reveal

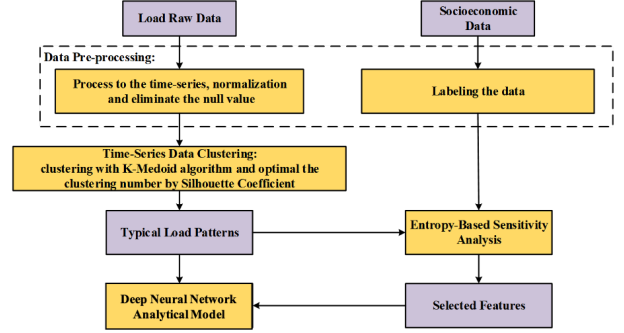


Figure 1: The flowchart of our study on the relationship between load patterns and socioeconomic factors.

the relationship between load patterns and socioeconomic factors using machine learning.

3. Load Patterns and Relationship with Socioeconomic Factors

In this section, we present our method to uncover the relationship between load patterns and socioeconomic factors. Figure 1 describes the flowchart of the proposed framework, and the details are presented in the following subsections.

- In Subsection 3.1, the consumption data are normalized to capture the temporal variations of daily time-series load, and the socioeconomic data are also processed.
- In Subsection 3.2, the typical load patterns are characterized by the K-Medoids clustering method, and the number of clusters is determined using the Silhouette Coefficient index.
- In Subsection 3.3, the socioeconomic features are selected based on their correlations with the clustered load patterns.
- In Subsection 3.4, we build a tailored analytical model with pattern-dependent deep neural networks and a normalization layer to study the relationship between load patterns and selected socioeconomic features.

3.1. Load Data Pre-processing and Socioeconomic Labels

Since the daily energy consumption is different on weekdays and weekends [35, 36], we divide the dataset into two groups for the workday and weekend per the date stamps. Specifically, we divide the load data of all the consumers (denoted as $\mathcal{N} = \{1, \dots, N\}$) into two parts: weekdays (denoted as w) and weekends (denoted as e). We denote D as the total number of days in the load data and each day is denoted as $d \in \{1, \dots, D\}$. Note that there are D_w days and D_e days in total for weekdays and weekends, respectively. Each day d is divided into 24 one-hour intervals, i.e., $t = 1, \dots, 24$. The load profile of consumer $n \in \mathcal{N}$ in hour t on day d is defined as $l_{w,d,t}^n$ and $l_{e,d,t}^n$ separately for weekdays and weekends. As we focus on the temporal variations of load, we normalize the original load profiles $l_{w,d,t}^n$ and

$l_{e,d,t}^n$ to be normalized ones $L_{w,d,t}^n$ and $L_{e,d,t}^n$ in the range of $[0, 1]$ shown as

$$L_{w,d,t}^n = \frac{l_{w,d,t}^n - \min_t\{l_{w,d,t}^n\}}{\max_t\{l_{w,d,t}^n\} - \min_t\{l_{w,d,t}^n\}}, \quad (1)$$

and

$$L_{e,d,t}^n = \frac{l_{e,d,t}^n - \min_t\{l_{e,d,t}^n\}}{\max_t\{l_{e,d,t}^n\} - \min_t\{l_{e,d,t}^n\}}, \quad (2)$$

where $\max_t\{l_{w,d,t}^n\}$ and $\min_t\{l_{w,d,t}^n\}$ (or $\max_t\{l_{e,d,t}^n\}$ and $\min_t\{l_{e,d,t}^n\}$) denote the maximum and minimum hourly load of consumer n on weekdays w (or weekends e) of day d .

For socioeconomic factors, it consists of different attributes, namely features, with various data types, shown as follows.

- *The number of residents in six different age ranges (integer variable);*
- *Annual income with ten ranges (categorical variable);*
- *Education level with four categories (categorical variable);*
- *Total square footage of the residents (integer variable).*

The ordered scales of the categorical variable are extracted into a matrix of metadata and expressed as the quantified ordinal classification. For the *annual income* and *education level*, the categories are labeled, as shown in Table 1.

Table 1: The Quantified Ordinal Classification of The Features

<i>Annual Income Range</i>	Value	<i>Education Level</i>	Value
Less than \$10,000	1	High School graduate	1
\$10,000 - 19,999	2		
\$20,000 - 34,999	3	Some college/trade /vocational school	2
\$35,000 - 49,999	4		
\$50,000 - 74,999	5		
\$75,000 - 99,999	6	College graduate	3
\$100,000 - 149,999	7		
\$150,000 - 299,000	8	Postgraduate degree	4
\$300,000 - 1,000,000	9		

3.2. Load Pattern Clustering by K-Medoids Algorithm

Real-world data samples often contain irregular data and outliers. As discussed, the conventional K-Means method is sensitive to outliers and noises, and the centroids can be greatly affected by outliers. Instead of finding centroids by the average, the K-Medoids method searches for the most central and representative sample in a cluster. It is also more robust to outliers and noises, compared with the K-Means method. Moreover, in our case, the K-Medoids algorithm derives clusters using actual load profiles rather than the mean of profiles and thus does not smooth out the temporal variations.

We use the K-Medoids method to characterize consumer load patterns, specifically by clustering the daily load profiles $L_{w,d}^n = (L_{w,d,t}^n, t = 1, \dots, 24)$ and $L_{e,d}^n = (L_{e,d,t}^n, t = 1, \dots, 24)$ of all consumers $n \in \mathcal{N}$ for weekdays and weekends, respectively. Without loss of generality, we assume that the K-Medoids algorithm is going to determine K clusters as load patterns on both

weekdays and weekends.¹ In the following, we take the clustering on weekdays as an example and use Euclidean distance measure for each pair of load profiles $i, j \in \{1, \dots, N \times D_w\}$ as

$$E_{i,j} = \|s_i - s_j\|, \quad (3)$$

where $s_i, s_j \in L_{w,d}^n$, and $d = 1, \dots, D_w$.

Based on the distance calculation, we use the K-Medoids algorithm in Algorithm 1 to obtain K representative load profiles $\hat{L}_w = \{\hat{L}_w^1, \dots, \hat{L}_w^K\}$ and a set of profile indices in each cluster denoted as $\hat{C}_w = \{\hat{C}_w^1, \dots, \hat{C}_w^K\}$. Specifically, we randomly select K load profiles from $L_{w,d}^n$ as the initial medoids. All the load profiles in $L_{w,d}^n$ are then separately calculated with the medoids based on the distance measure. For the initial K medoids, the shortest distance between the profile and the medoid determines the allocation of each profile in the nearest cluster as described in step 4. In step 5, the cluster score is defined as the summation of the total distance between each profile to its medoid. Afterward, the algorithm proceeds iteratively from step 6 to 12. Each iteration begins with the pairwise distance measurements among the profiles in the same cluster. The profile, having the overall shortest distance with the rest of others in the same cluster, is updated to be the new medoid.

We update the cluster referring to the new medoid and repeat all the steps to assign all load profiles in the corresponding clusters based on the shortest-distance rule. At each iteration denoted as *iter*, $L_w^{(iter)}$ and $C_w^{(iter)}$ are employed to store the temporary results for \hat{L}_w and \hat{C}_w . The iterations end once the cluster score does not decrease. The algorithm outputs the medoids in \hat{L}_w representing the major load patterns on weekday and \hat{C}_w containing the profile indices corresponding to each pattern. Similarly, we can obtain the weekend load patterns \hat{L}_e and the index set \hat{C}_e using Algorithm 1 based on the weekend load profiles $L_{e,d}^n$.

Despite the advantage of robustness, there still exists a problem for K-Medoids clustering being widely discussed, e.g., a heavy computational overhead. As defined in (3), the pairwise calculation is required in K-Medoids clustering, which directly causes high overhead with a large number of data samples. Therefore, we adopt an improved K-Medoids algorithm, *trimed*, [37] to enhance the computational efficiency. The improved algorithm *trimed* can reduce the computational complexity from $O(N^2)$ to $O(N^{3/2})$.

We further investigate how to determine the value of K using the Silhouette Coefficient index [38]. Specifically, the Silhouette Coefficient index SC consists of two parts: the cohesion factor a_i and the separation factor b_i , which are defined as

$$a_i = \frac{\sum_{j \in \hat{C}_w^k \setminus i} E_{i,j}}{M_w^k - 1}, \quad (4)$$

$$b_i = \min_{k' \in \{1, \dots, K\} \setminus k} \frac{\sum_{j \in \hat{C}_w^{k'}} E_{i,j}}{M_w^{k'}} \quad (5)$$

¹We will discuss how to select the number of clusters K at the later part from Eq. (4) of Section 3.

Algorithm 1: Load Clustering Algorithm.

Input: The number of clusters K and the total daily load profiles $L_{w,d}^n$
Output: The K representative load pattern \hat{L}_w and index set \hat{C}_w

- 1 Iteration time $iter = 0$;
- 2 Randomly select K load profiles from $L_{w,d}^n$ as the initial medoids $L_w^{(iter)}$;
- 3 For each profile i , determine its belonging $C_w^{(iter)}$ per the shortest distance to the medoids, i.e.,
 $\arg \min_{k \in \{1, \dots, K\}} \|s_i - L_w^{k,(iter)}\|$, where $s_i \in L_{w,d}^n$;
- 4 and $s_j \in L_w^{(iter)} = \{\hat{L}_w^1, \dots, \hat{L}_w^K\}$;
- 5 $ClusterScore^{(iter)} = \sum_{k=1}^K \sum_{i \in C_w^{k,(iter)}} \|s_i - L_w^{k,(iter)}\|$;
- 6 **for** Iteration time $iter \leq iter^{max}$ **do**
- 7 $iter = iter + 1$;
- 8 Update $L_w^{k,(iter)}$ with the profile whose index in $C_w^{k,(iter-1)}$ through $\arg \min_i \sum_{j \in C_w^{k,(iter-1)}} E_{i,j}$;
- 9 Update $C_w^{k,(iter)}$ refer to Step 3 ;
- 10 Update $ClusterScore^{(iter)}$ refer to Step 4 ;
- 11 **if** $ClusterScore^{(iter)} = ClusterScore^{(iter-1)}$ **then**
- 12 | break;
- 13 $\hat{L}_w = L_w^{(iter)}$, $\hat{C}_w = C_w^{(iter)}$

where $k = 1, \dots, K$, and M_w^k represents the number of load profile indices in \hat{C}_w^k . Factor a_i stands for the mean distance between the i -th load profile and other load profiles in the same cluster k . Factor b_i measures i -th load profile's minimum averaged distance to load profiles of other load clusters $k' \in \{1, \dots, K\} \setminus k$.

Then we obtain SC_i for load profile i as

$$SC_i = \frac{b_i - a_i}{\max(b_i, a_i)}, \quad (6)$$

which is employed to estimate whether the assignment of the i -th load profile is appropriate. A smaller cohesion factor a_i and a larger separation factor b_i are preferred.

The overall clustering performance is thus measured by SC as

$$SC = \frac{\sum_{i=1}^{M_w} SC_i}{M_w}, \quad (7)$$

which is ranged within $[-1, 1]$ and $M_w \triangleq N \times D_w$. A higher Silhouette Coefficient index determines a better descriptive number of K .

After obtaining the major load patterns, we further calculate the load pattern distribution of consumer n in pattern k by

$$p_{k,n} = \frac{M_{k,n}}{\sum_{k=1}^K M_{k,n}}, \quad (8)$$

where the number of load profiles of consumer n in the k -th cluster denoted as $M_{k,n}$. We will use $p_{k,n}$ together with consumers' socioeconomic factors to further study their correlations.

3.3. Load Pattern-Related Socioeconomic Features Selection

Real-world data often contain irrelevant and redundant features as well and thus can cause low accuracy, unnecessarily complex modeling, and high computational burden for prediction models. Feature selection plays a key role in eliminating redundant features and selecting the best subset of predictors (i.e., features) [38]. With the determined load patterns in Subsection 3.2, we explore the correlations between the socioeconomic features and the load patterns.

In this subsection, we present how to select socioeconomic features via an entropy-based filter method. In our problem, the socioeconomic features include different types, e.g., *age*, *education*, *income*, and *household square footage*, but how these features are correlated with each load pattern remains unknown. Therefore, we use feature selection techniques to identify the relevant features for the prediction of the distribution of load patterns. Specifically, the entropy-based class measurement [33], which has been widely employed in filter models [31], is used in this paper.

We define the set of features, including *the number of residents in each age range*, *annual income*, *educational level*, and *the total foot square*, as \mathcal{S} . We aim to select a subset of features $\mathcal{S}^k \subseteq \mathcal{S}$ for each load pattern k to minimize the redundancy. To determine the best subset \mathcal{S}^k , we evaluate all combinations of features $\mathcal{S}' \subseteq \mathcal{S}$. The entropy-based methodology measures the intercorrelation among the features in \mathcal{S}' pairwise and the correlations between features in \mathcal{S}' and predicted target, i.e., the percentage/probability of the user's load profiles in pattern cluster k denoted by $\mathbf{p}_k = (p_{k,n}, n = 1, \dots, N)$. Then the subset with the highest measurement value is determined to be \mathcal{S}^k , which selects the features having a high correlation with the evaluating target.

We denote \mathcal{U} and \mathcal{V} as two different features in \mathcal{S}' . For example, the features *number of resident age under 13* and *education level* can form the feature subset \mathcal{S}' . We let $\mu_n \in \mathcal{U}$ and $v_n \in \mathcal{V}$ denote randomly selected feature values for consumer $n \in \mathcal{N}$ from \mathcal{U} and \mathcal{V} , respectively. For the *number of resident age under 13*, the value of μ_n can be '0', '1', or other integers. If the underlying feature is the *education level*, the corresponding values are '1', '2', '3', and '4' representing four education levels from the high school to graduate school.

We denote $P(\mu_n)$ and $P(v_n)$ as the marginal probabilities for the feature values. The marginal probability $P(\mu_n = 0)$ of the feature *number of resident age under 13* therefore represents the statistical probability of value '0' among all the possible realizations for the underlying feature. Similar to the marginal probability $P(\mu_n)$, the joint probability $P(\mu_n, v_n)$, represents the statistical probability of the value μ_n and v_n appearing at the same time in \mathcal{U} and \mathcal{V} .

The entropy $H(\mathcal{U})$, as a measure of distribution property, is calculated based on $P(\mu_n)$ by

$$H(\mathcal{U}) = - \sum_{\mu_n \in \mathcal{U}} P(\mu_n) \log P(\mu_n), \quad (9)$$

where $H(\mathcal{U})$ ranges from 0 to 1. The higher level of disorder of data in \mathcal{U} corresponds to a greater value of $H(\mathcal{U})$. Based on

the idea of entropy evaluation and the joint probability, mutual information $MI(\mathcal{U}, \mathcal{V})$ is a technique to measure how much knowledge between two features is correlated. It is defined as the difference between the sum of the marginal entropy and their joint entropy [39] and written as

$$MI(\mathcal{U}, \mathcal{V}) = \sum_{\mu_n \in \mathcal{U}} \sum_{v_n \in \mathcal{V}} P(\mu_n, v_n) \log \frac{P(\mu_n, v_n)}{P(\mu_n)P(v_n)}. \quad (10)$$

Note that dependency $MI(\mathcal{U}, \mathcal{V})$ reflects the correlation of the features and is always nonnegative. It is zero if and only if \mathcal{U} and \mathcal{V} are independent. A stronger dependency between \mathcal{U} and \mathcal{V} is revealed when $MI(\mathcal{U}, \mathcal{V})$ is relatively large.

The symmetric uncertainty (SU) is one of the normalized forms of MI and is defined as

$$SU(\mathcal{U}, \mathcal{V}) = 2 \frac{MI(\mathcal{U}, \mathcal{V})}{H(\mathcal{U}) + H(\mathcal{V})}, \quad (11)$$

where SU ranges in $[0, 1]$. The value '1' indicates the knowledge of \mathcal{U} completely predicts that of \mathcal{V} where the value '0' indicating that \mathcal{U} and \mathcal{V} are independent. Similarly, the target-related SU , e.g., $SU(\mathcal{U}, p_k)$, is calculated to estimate the correlation between the feature \mathcal{U} and target p_k .

Finally, based on the calculated symmetric uncertainty, we select the subset of features \mathcal{S}^k as

$$\mathcal{S}^k = \arg \max_{\mathcal{S}' \subseteq \mathcal{S}} \frac{\sum_{\mathcal{U} \in \mathcal{S}'} SU(\mathcal{U}, p_k)}{\sqrt{\sum_{\mathcal{U} \in \mathcal{S}'} \sum_{\mathcal{V} \in \mathcal{S}'} SU(\mathcal{U}, \mathcal{V})}}, \quad (12)$$

where \mathcal{S}^k is determined to select the feature(s) that are highly correlated with the target but less correlated with each other. For each load pattern k , we run Equation (12) over all combinations of feature $\mathcal{S}' \subseteq \mathcal{S}$ to obtain \mathcal{S}^k . The K selected feature subsets are finally obtained as $\{\mathcal{S}^k, k = 1, \dots, K\}$ and will be used as the indicators in the analytical model in Section 3.4.

3.4. The Relationship Between Load Patterns and Socioeconomic Factors

Deep learning has been successfully used many energy studies, and the authors in [40] reviewed the research on deep learning applications to demand and renewable generation prediction, DR, and anomaly detection. Different from these studies, we develop a DNN-based analytical model to uncover the relationship between the load patterns and socioeconomic factors. Thanks to the Pecan Street project [22], both household-level load data and socioeconomic data are made available and thus enable our work.

From Section 3.3, we obtained the selected features \mathcal{S}^k for each load pattern k . Accordingly, we build K different DNN models with \mathcal{S}^k as the input to estimate the probability distribution of load pattern k . However, in this way, the property of the probability distribution can not be always satisfied, and we introduce a normalization layer. The structure of the model, represented in Fig. 2, is constructed with three components, e.g., pattern-dependent deep analytical networks, normalization layer, and output layer.

We employ a DNN model for each load pattern k in the networks with the pattern-corresponding feature set \mathcal{S}^k as the

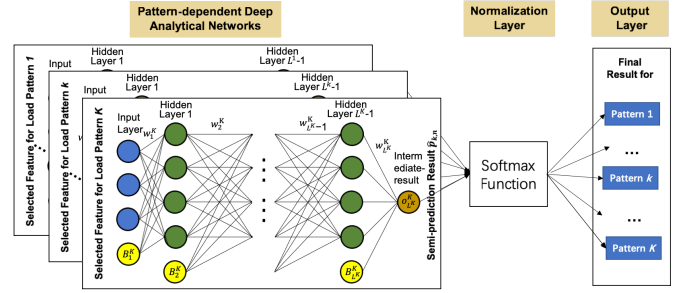


Figure 2: The structure of the joint DNN model for revealing the relationship between load patterns and socioeconomic factors.

input, namely pattern-dependent deep analytical networks as shown in Figure 2. The structure including weights and biases of each DNN model is identical. We take the k -th DNN model as an example. In the model, we aim to map the value of features in \mathcal{S}^k belonging to consumer n onto the pattern distribution value $p_{k,n}$. Concretely, for each layer $l \in \{1, \dots, L^k\}$, the outputs in the $(l-1)$ -th layer are computed with the weights w_l^k through the inner product operation and then passed through a pre-defined activation function with bias B_l^k . The calculation,

$$o_l^k = \sigma((w_l^k)^\top o_{l-1}^k + B_l^k), \quad (13)$$

generates the scalar state o_l^k , which is also named as the output of layer l . We use the sigmoid function for the activation function $\sigma(\cdot)$. We name the output of the last layer $o_{L^k}^k$ the intermediate-result of the analysis, which is defined as $\hat{p}_{k,n}$. As each $\hat{p}_{k,n}$ is obtained distinctly, the intermediate-results in vector $\hat{\mathbf{p}}_n = [\hat{p}_{1,n}, \dots, \hat{p}_{K,n}]$ can not be always in the range of $[0, 1]$, while the summation of the prediction of a certain consumer n cannot be ensured to be consistently 1.

The normalization layer is thus used to enforce the property of the probability distribution after the intermediate-result $\hat{\mathbf{p}}_n$ is generated. The softmax function [41], as a popular normalization algorithm, is employed to transform the input vector $\hat{\mathbf{p}}_n$ into $\hat{\mathbf{p}}_n^* = [\hat{p}_{1,n}^*, \dots, \hat{p}_{K,n}^*]$ as

$$\hat{p}_{k,n}^* = \frac{e^{\hat{p}_{k,n}}}{\sum_{k=1}^K e^{\hat{p}_{k,n}}}, \quad (14)$$

whose value satisfies the property of probability distribution. The output $\hat{p}_{k,n}^*$ is defined as the evaluated percentage of user n 's load profiles in k -th load pattern. The normalization layer guarantees that the evaluated probabilities $\hat{p}_{k,n}^*$ are non-negative and within $[0, 1]$, and their summation is 1. During the training stage, $\hat{p}_{k,n}^*$ is used to define the loss function for the k -th pattern-dependent deep network.

We use the mean squared error (MSE) as the loss function to train K DNN models in parallel. By measuring the dissimilarity between the original probability $p_{k,n}$ and $\hat{p}_{k,n}^*$, the loss function is calculated by

$$MSE_k = \sqrt{\frac{1}{N'} \sum_{n=1}^{N'} (p_{k,n} - \hat{p}_{k,n}^*)^2}, \quad (15)$$

where N' is the number of consumers randomly selected to train the model from the N consumers. Stochastic gradient descent method is introduced to train and update the weight w_l^k and bias B_l^k in the back-propagation way. And the training stops when MSE is below some threshold or the number of iterations or epochs is above some threshold.

To show the improvement made by our proposed analytical scheme, we compare our model with a regression model and two DNN-based models as benchmarks:

- *Benchmark 1* employs XGBoost to construct a non-linear regression model. The model is to describe the relationship between the selected features with non-selected features in \mathcal{S} as the indicator.
- *Benchmark 2* uses a single DNN model to using non-selected features in \mathcal{S} as inputs.
- *Benchmark 3* has the same structure of our analytical model, as shown in Fig. 2, but takes non-selected features in \mathcal{S} as inputs.

The comparison results will be present in the following section.

4. Simulation Results and Discussions

This section presents the load patterns clustered by the K-Medoids algorithm for weekdays and weekends, respectively. Then we select features using the entropy-based algorithm and employ Pearson correlation to further interpret the result. Last but not least, the overall performance of our proposed analytical model is validated through comparisons with three benchmarks. Before presenting the numerical results, we describe the data used in this work. We use the smart meter data in 2019 and socioeconomic information from Pecan Street [22]. After pre-processing the data, we selected 433 households with the complete hourly consumption for three years (2015-2017) and the corresponding socioeconomic information.

4.1. Load Pattern by Clustering

We evaluate the clustering performance of the K-Medoids method under different values of K and calculate the Silhouette Coefficient by Equation (7). The results are represented as the average values of ‘weekday’ and ‘weekend’ load clustering in Fig. 3. We see that the K-Medoids method has distinct values of the Silhouette Coefficient with respect to K . The clustering result with $K = 6$ performs the best with the highest average value for both weekday and weekend. Meanwhile, $K = 3$ also demonstrates a high value. However, considering the interpretability of the clustering results, we choose $K = 6$. In the following discussion, we represent 6 load patterns on weekdays and weekends and distinguish G1-G6 for weekdays and weekends by ‘W’ and ‘E’, respectively.

We show the clustered load patterns in Fig. 4 for weekdays and Fig. 5 for weekends, where the blue dash lines display the medoids and the grey lines depict all load profiles in the corresponding cluster. The main difference between weekday and weekend load patterns lies in the load shape, especially in peak

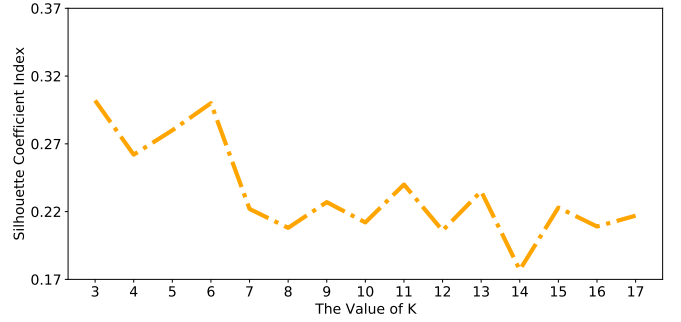


Figure 3: The SC index according to the change of K .

Table 2: The Selected Feature for Each Load Pattern

Feature	Weekday						Weekend					
	G1	G2	G3	G4	G5	G6	G1	G2	G3	G4	G5	G6
Number of Resident Age Range	under 12											
	13-24											
	25-49											
	50-64											
	over 65											
Education Level												
Annual Income												
Total Square Footage												

time. We see that all 6 medoids on weekdays have evening peaks. On the contrary, we find that the shapes of load patterns on the weekend are more diverse, e.g., peaks in both daytime and evening, and relatively higher consumption during the daytime, indicating less routine household activities on weekends.

Meanwhile, we show the percentage of consumers’ daily load profiles belonging to each load pattern in Fig. 6. For the load patterns on weekdays, we see that G1, G2, and G3 are the most representative load patterns covering 60% of load profiles. This indicates a lifestyle of consumers in general that residents leave home in the morning, come back from work or school in the evening, and the energy consumption goes to a daily peak until sleeping. Note that the main difference among G1, G2, and G3 is the peak time. As two relatively rare consumption types, G5 and G6 cover 13.5% and 12.1% of weekday load profiles. Compared with G1-G3, G5 and G6 have higher consumption during the daytime, implying regular occupancy in the daytime on weekdays. The distribution of load patterns on weekend can also be found in Fig. 6(b). We see that G4, G5, and G6 are the most representative load patterns on weekends. Compared with the top three representative load patterns on weekdays, those on weekends have a single peak or dual peak during 9:00-18:00.

4.2. Pattern-Related Feature Selection

In this subsection, we show the selected socioeconomic features for each load pattern. All the features in the original set \mathcal{S} are listed in the first column of TABLE 2. Applying the feature selection method presented in Section 3.3, we obtain the selected features in \mathcal{S}^k that are marked.

We see that for all the load patterns, no matter on weekdays or weekends, the most related feature(s), i.e., the ones in \mathcal{S}^k , are very different. Taking G1(W) and G2(W) as an example, two

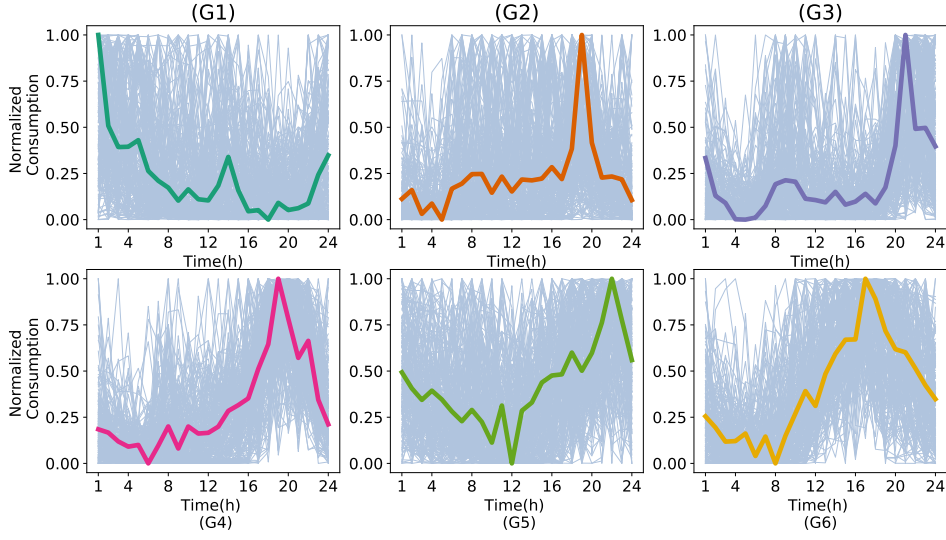


Figure 4: The six load patterns for weekdays.

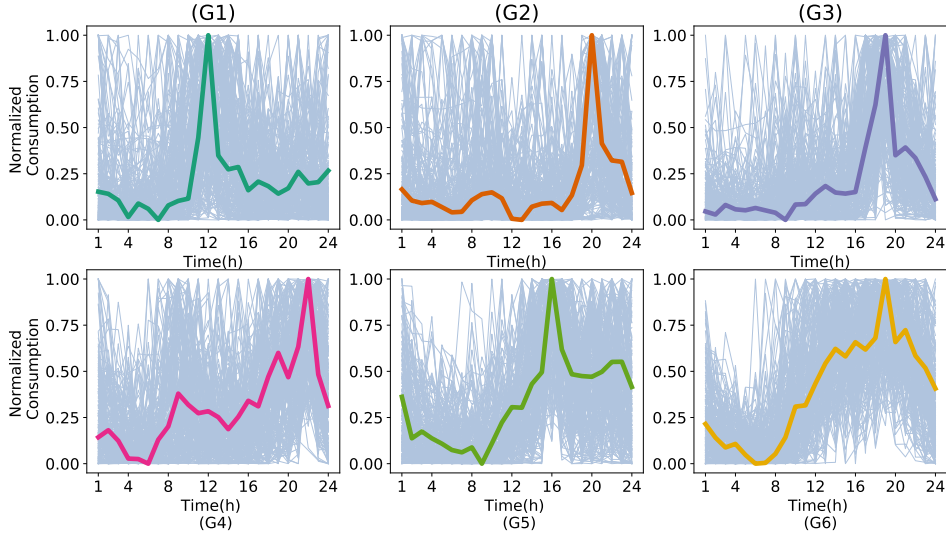


Figure 5: The six load patterns for weekends.

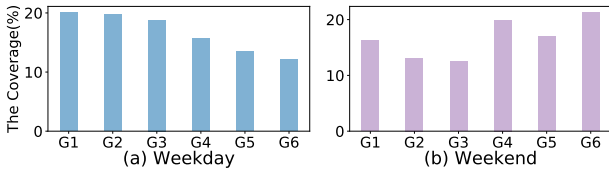


Figure 6: The percentage distribution for load patterns on Weekdays and Weekends.

features, e.g., *Age Over 65* and *Education Level*, are selected simultaneously for $\mathcal{S}^{G1(W)}$ and $\mathcal{S}^{G2(W)}$, but the feature *age under 12* is selected in $\mathcal{S}^{G2(W)}$ alone. The diverse pattern-related feature sets reveal the importance of the feature-dependant design for the prediction model. In addition, age and education are highly influencing features, suggesting that age and education help determine the load patterns. Specifically, we find that the age greater than 65 exhibits a high correlation with load patterns on weekdays. Meanwhile, on weekends, the age ranging from 12 to 49 has a higher impact on the load pattern. Besides, the education level shows a strong impact on all the load patterns. In contrast, the feature *Total Square Footage* does not show a strong correlation with any load patterns, because the

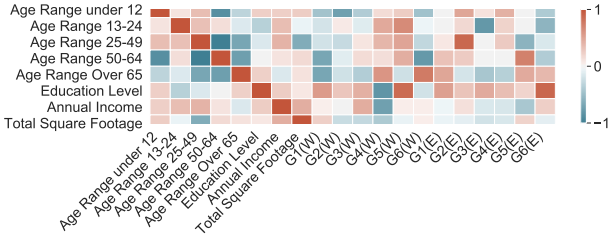


Figure 7: The Pearson correlation coefficient between the features and load patterns.

load profiles have been normalized in this study. The selected features for load patterns on weekdays and weekends are different, which justifies the need to consider weekday and weekend load patterns separately.

4.3. The Correlation Coefficient between The Features

We further use Pearson correlation coefficient to provide more insights into the pairwise correlation not only between the features and load patterns but also among different features. The coefficients represent the dependence of the relationship, while the sign exhibits a positive or negative correlation. We create a heatmap to visualize the correlations in Fig. 7, in which we use the red gradient color for varying degrees of positive correlations and blue for negative correlations. Taking the feature *Age Range Over 65* as an example, it has a negative correlation with *Age Range 50-64* and *Age Range 25-49*, which indicate that the residents from these three age ranges are unlikely to live in the same household. Given such a strong correlation, the feature *Age Range Over 65* is thus selected as the other two features are redundant. The selected features for G1(W) are consistent with this analysis. Even though *Age Range 50-64* shows a strong correlation with G1(W) in the heatmap, it is not selected in TABLE 2. The above results also validate the employed feature selection method that does count in the correlation measurement and apparent redundancy.

4.4. Load Patterns and Socioeconomic Factors

We take the selected features in TABLE 2 as the inputs of our analytical model presented in Section 3.4 to reveal the corresponding probability distributions of load patterns. For both weekday and weekend data, we use 70% of the data for training, 15% for validation, and the remaining 15% for the test. By applying grid search [42] on the validation dataset and MSE as the evaluator, we optimize the hyper-parameters, e.g., set 5 layers and 1024 neurons for each layer.

4.4.1. Individual Households

We select three households (#59, #434, and #4310) from the dataset [22] to show the test results, and the household information is listed in Table 3. The three households have diverse socioeconomic features, including two seniors with high education levels and income in household #59, a family of two children and two adults with medium income in household #434, and three adults with the college education and modest income

Table 3: The Information of Three Selected Households

Socioeconomic Information		Consumer ID		
		#59	#434	#4310
Age Range	under 12	0	2	0
	13-24	0	0	2
	25-49	0	2	0
	50-64	0	0	1
	over 65	2	0	0
Education Level	Postgraduate Degree	Postgraduate Degree	College Graduate	
Annual Income (\$)	300,000 - 1,000,000	150,000 - 299,000	100,000 - 149,999	
Total Square Footage (ft^2)	3830	2160	3130	

in household #4310. The results are depicted in the radar maps of Fig. 8, illustrating the estimated distributions of load patterns for our model and three benchmarks.

We see in Fig. 8 that the regression results (in orange dash-line) using our proposed method best match the ground truth (in red line) for all three case studies on weekdays and weekends. In contrast, Benchmark 1's results (in blue dash-line) deviate from the ground truth significantly in all the cases, suggesting that the regression model is underfitting. Benchmark 2's results (in green dash-line) and Benchmark 3's results (in purple dash-line) are better than that of Benchmark 1 but not competitive to our proposed method. Specifically, significant inaccuracy occurs in Benchmark 2 for #59 and #4310 on the weekend.

The results reveal rich information about how different households consume energy. For example, Household #59 has two elderly residents with high education levels and high incomes. They have a stable consumption behavior with three major load patterns in G1, G3, and G5. On weekdays, they may cook lunch leading to a midday peak in G1(W), getting up early in the morning and cook dinner in G3(W), or stay at home with high consumption in the afternoon followed by a night peak in G5(W). During the weekend, the dominant pattern G1(E) indicates that they have a midday peak, suggesting energy-intensive household activities. They also have energy-intensive household activities in the afternoon (G5(E)) or for dinner (G3(E)). Similarly, the load patterns of Households #434 and #4310 can be explained.

4.4.2. Overall Performance

We also use MSEs in Equation (15) to measure the errors of all compared methods, as shown in TABLE 4 for both weekdays and weekends. Benchmark 1 does not perform well on both weekdays and weekends. Employing DNN, Benchmark 2 obtains a noticeable improvement compared with Benchmark 1. However, using our proposed DNN structure, both benchmark 3 and our model significantly reduce the errors by 42.5% and 54.2% compared with Benchmark 2. Using feature selection, our model achieves a further reduction of 20.4% in errors compared to Benchmark 3. Moreover, as the *ClusterScore* for the weekend load pattern is lower than that for the weekday load pattern, the overall MSE for weekends is lower than weekdays.

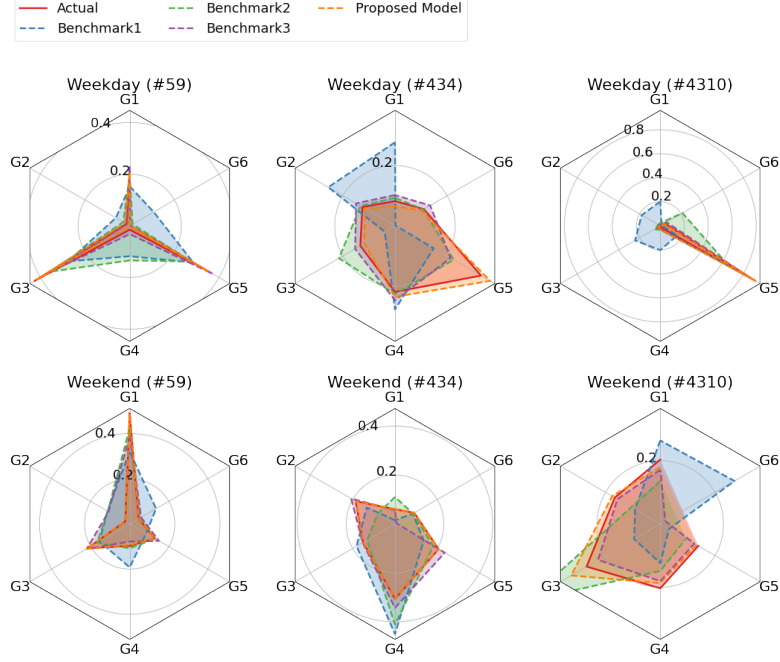


Figure 8: Comparison of our model and three benchmarks for estimating load pattern distributions of three households (#59, #434, and #4310).

Table 4: The Average MSE Comparison between The Models

Analytical Model	Average MSE	Error Reduction Compared with (%)		
		Benchmark1	Benchmark2	Benchmark3
Weekday				
Benchmark 1	0.134			
Benchmark 2	0.038	71.6		
Benchmark 3	0.022	83.6	42.5	
Proposed Model	0.017	87.3	54.2	20.4
Weekend				
Benchmark 1	0.072			
Benchmark 2	0.012	83.7		
Benchmark 3	0.010	86.5	16.7	
Proposed Model	0.009	87.8	23.0	7.0

Note that the performance in terms of errors will be affected by data, and we do not intend to emphasize on percentage improvement made by our model. Instead, the results demonstrate that our model better captures the nonlinearity between the load pattern and socioeconomic features.

5. Conclusion

We developed an analytical method to advance the understanding of residential electricity load patterns by focusing on the impact of consumers' socioeconomic factors. Specifically, we used K-Medoid clustering to identify representative load patterns, given K-Medoid's advantage of being robust to outliers. We also used the entropy-based feature selection method to obtain the pattern-related feature sets. The feature selection

contributed to identifying the critical socioeconomic factors on different load patterns and improving the interpretability of our method. Then we developed a deep learning model to reveal the relationship between the distribution of load patterns and the selected socioeconomic features. Our model consists of pattern-dependent DNNs and a normalization layer to enhance the accuracy. Our model consists of pattern-dependent DNNs and a normalization layer to enhance the accuracy. We summarize the results based on the realistic load data and socioeconomic data as follows.

1. We obtained 6 representative daily load curves to model the consumption patterns of weekdays, and all 6 load curves showed evening peaks. Also, 6 daily load curves were selected to model the consumption on weekends, and

a single peak or dual peaks during 9:00-18:00 were more commonly found.

2. The age and education level were found to be two significant drivers of load patterns. Meanwhile, the education level has a strong effect on all load patterns.
3. It can be observed that consumers with age older than 65 make a great impact on the weekdays' typical consumption curves. The people aged older than 65 are thus potentially the target participants in demand response programs.
4. The rich information can be revealed by the DNN model through analyzing how individual household consumes energy and how diverse socioeconomic factors make the effect on the consumption.
5. The comparison results with other benchmark methods show the non-linear relationship between the selected features and load patterns. Our model is better at mapping the socioeconomic features to the load patterns with an average error reduction of 46.5% compared to benchmark methods.

For our future work, we plan to

1. study appliance consumption data and consider categories, e.g., season, holiday, or different weather;
2. analyze the price elasticity of the consumption by considering price factors as the inputs of the DNN model;
3. and further develop energy programs, such as demand response, using the results of the consumers' load pattern probabilities.

References

- [1] A. Barbato, A. Capone, M. Rodolfi, D. Tagliaferri, Forecasting the usage of household appliances through power meter sensors for demand management in the smart grid, in: 2011 IEEE International Conference on Smart Grid Communications, IEEE, 2011, pp. 404–409.
- [2] L. M. Candanedo, V. Feldheim, D. Deramaix, Data driven prediction models of energy use of appliances in a low-energy house, *Energy and Buildings* 140 (2017) 81–97.
- [3] H. Shi, M. Xu, R. Li, Deep learning for household load forecasting—a novel pooling deep rnn, *IEEE Transactions on Smart Grid* 9 (2017) 5271–5280.
- [4] Y. Wang, Q. Chen, T. Hong, C. Kang, Review of smart meter data analytics: Applications, methodologies, and challenges, *IEEE Transactions on Smart Grid* 10 (2018) 3125–3148.
- [5] S. Lin, F. Li, E. Tian, Y. Fu, D. Li, Clustering load profiles for demand response applications, *IEEE Transactions on Smart Grid* 10 (2019) 1599–1607.
- [6] M. Sun, Y. Wang, F. Teng, Y. Ye, G. Strbac, C. Kang, Clustering-based residential baseline estimation: A probabilistic perspective, *IEEE Transactions on Smart Grid* 10 (2019) 6014–6028.
- [7] S. Ryu, H. Choi, H. Lee, H. Kim, Convolutional autoencoder based feature extraction and clustering for customer load analysis, *IEEE Transactions on Power Systems* 35 (2019) 1048–1060.
- [8] Z. Niu, J. Wu, X. Liu, L. Huang, P. S. Nielsen, Understanding energy demand behaviors through spatio-temporal smart meter data analysis, *Energy* 226 (2021) 120493.
- [9] Z. Wang, J. Crawley, F. G. Li, R. Lowe, Sizing of district heating systems based on smart meter data: Quantifying the aggregated domestic energy demand and demand diversity in the uk, *Energy* 193 (2020) 116780.
- [10] V. Azarova, D. Engel, C. Ferner, A. Kollmann, J. Reichl, Exploring the impact of network tariffs on household electricity expenditures using load profiles and socio-economic characteristics, *Nature Energy* 3 (2018) 317–325.
- [11] J. Kwac, J. I. Kim, R. Rajagopal, Efficient customer selection process for various dr objectives, *IEEE Transactions on Smart Grid* 10 (2017) 1501–1508.
- [12] J. Kwac, J. Flora, R. Rajagopal, Household energy consumption segmentation using hourly data, *IEEE Transactions on Smart Grid* 5 (2014) 420–430.
- [13] J. Kwac, J. Flora, R. Rajagopal, Lifestyle segmentation based on energy consumption data, *IEEE Transactions on Smart Grid* 9 (2016) 2409–2418.
- [14] A. Capozzoli, M. S. Piscitelli, S. Brandi, D. Grassi, G. Chicco, Automated load pattern learning and anomaly detection for enhancing energy management in smart buildings, *Energy* 157 (2018) 336–352.
- [15] Y. Wang, Q. Chen, C. Kang, Q. Xia, Clustering of electricity consumption behavior dynamics toward big data applications, *IEEE transactions on smart grid* 7 (2016) 2437–2447.
- [16] J. Kwac, R. Rajagopal, Data-driven targeting of customers for demand response, *IEEE Transactions on Smart Grid* 7 (2015) 2199–2207.
- [17] R. V. Jones, A. Fuertes, K. J. Lomas, The socio-economic, dwelling and appliance related factors affecting electricity consumption in domestic buildings, *Renewable and Sustainable Energy Reviews* 43 (2015) 901–917.
- [18] T.-H. Dang-Ha, R. Olsson, H. Wang, The role of big data on smart grid transition, in: 2015 IEEE International Conference on Smart City/SocialCom/SustainCom (SmartCity), IEEE, 2015, pp. 33–39.
- [19] J. D. Rhodes, W. J. Cole, C. R. Upshaw, T. F. Edgar, M. E. Webber, Clustering analysis of residential electricity demand profiles, *Applied Energy* 135 (2014) 461–471.
- [20] W. Tang, X. Lee, H. Wang, H. Yang, Leveraging socioeconomic information and deep learning for residential load pattern prediction, in: 2019 IEEE PES Innovative Smart Grid Technologies Europe (ISGT-Europe), 2019, pp. 1–5.
- [21] L. Li, H. Ming, W. Fu, Q. Shi, S. Yu, Exploring household natural gas consumption patterns and their influencing factors: An integrated clustering and econometric method, *Energy* 224 (2021) 120194.
- [22] Pecan Street, Pecan street online database, 2019. URL: <https://www.pecanstreet.org/work/energy/>, accessed: July 2019.
- [23] X. Ruhang, Efficient clustering for aggregate loads: An unsupervised pretraining based method, *Energy* 210 (2020) 118617.
- [24] O. Motlagh, A. Berry, L. O'Neil, Clustering of residential electricity customers using load time series, *Applied Energy* 237 (2019) 11–24.
- [25] I. J. Scott, P. M. Carvalho, A. Botterud, C. A. Silva, Clustering representative days for power systems generation expansion planning: Capturing the effects of variable renewables and energy storage, *Applied Energy* 253 (2019) 113603.
- [26] H.-S. Park, C.-H. Jun, A simple and fast algorithm for k-medoids clustering, *Expert Systems with Applications* 36 (2009) 3336–3341.
- [27] J. P. Gouveia, J. Seixas, G. Long, Mining households' energy data to disclose fuel poverty: Lessons for southern europe, *Journal of Cleaner Production* 178 (2018) 534–550.
- [28] Y. Han, X. Sha, E. Grover-Silva, P. Michiardi, On the impact of socioeconomic factors on power load forecasting, in: IEEE International Conference on Big Data (Big Data), IEEE, 2014, pp. 742–747.
- [29] A. Kavousian, R. Rajagopal, M. Fischer, Determinants of residential electricity consumption: Using smart meter data to examine the effect of climate, building characteristics, appliance stock, and occupants' behavior, *Energy* 55 (2013) 184–194.
- [30] L. Yu, H. Liu, Feature selection for high-dimensional data: A fast correlation-based filter solution, in: Proceedings of the 20th international conference on machine learning (ICML-03), 2003, pp. 856–863.
- [31] I. H. Witten, E. Frank, M. A. Hall, C. J. Pal, *Data Mining: Practical machine learning tools and techniques*, Morgan Kaufmann, 2016.
- [32] A. Bommert, X. Sun, B. Bischl, J. Rahnenführer, M. Lang, Benchmark for filter methods for feature selection in high-dimensional classification data, *Computational Statistics & Data Analysis* 143 (2020) 106839.
- [33] S. Jurado, A. Nebot, F. Mugica, N. Avellana, Hybrid methodologies for electricity load forecasting: Entropy-based feature selection with machine learning and soft computing techniques, *Energy* 86 (2015) 276–291.

- [34] J. L. Viegas, S. M. Vieira, R. Melício, V. Mendes, J. M. Sousa, Classification of new electricity customers based on surveys and smart metering data, *Energy* 107 (2016) 804–817.
- [35] S. Zhang, J. Lian, Z. Zhao, H. Xu, J. Liu, Grouping model application on artificial neural networks for short-term load forecasting, in: 2008 7th World Congress on Intelligent Control and Automation, IEEE, 2008, pp. 6203–6206.
- [36] Y. Wang, Q. Chen, C. Kang, M. Zhang, K. Wang, Y. Zhao, Load profiling and its application to demand response: A review, *Tsinghua Science and Technology* 20 (2015) 117–129.
- [37] J. Newling, F. Fleuret, A sub-quadratic exact medoid algorithm, in: *Artificial Intelligence and Statistics*, PMLR, 2017, pp. 185–193.
- [38] L. Zhu, B. Ma, X. Zhao, Clustering validity analysis based on silhouette coefficient, *Journal of Computer Applications* 30 (2010) 139–141.
- [39] E. Sarhrouni, A. Hammouch, D. Aboutajdine, Application of symmetric uncertainty and mutual information to dimensionality reduction and classification of hyperspectral images, *arXiv preprint arXiv:1211.0613* (2012).
- [40] D. Zhang, X. Han, C. Deng, Review on the research and practice of deep learning and reinforcement learning in smart grids, *CSEE Journal of Power and Energy Systems* 4 (2018) 362–370. doi:10.17775/CSEEJPES.2018.00520.
- [41] G. Bouchard, Efficient bounds for the softmax function, applications to inference in hybrid models, in: *Workshop for Approximate Bayesian Inference in Continuous/Hybrid Systems at NIPS-07*, Citeseer, 2007.
- [42] J. S. Bergstra, R. Bardenet, Y. Bengio, B. Kégl, Algorithms for hyperparameter optimization, in: *Advances in neural information processing systems*, 2011, pp. 2546–2554.